




## Availability of water glass/ $\text{Bi}_2\text{O}_3$ composites in dielectric and gamma-ray screening applications

Tuğba Demirbay<sup>a</sup>, Mustafa Çağlar<sup>b</sup>, Yaşar Karabul<sup>a</sup>, Mehmet Kılıç<sup>a</sup>, Orhan İçelli<sup>a</sup> and Zeynep Güven Özdemir <sup>a</sup>

<sup>a</sup>Department of Physics, Yıldız Technical University, Istanbul, Turkey; <sup>b</sup>Department of Medical Physics, Institute of Health Sciences, Istanbul Medipol University, Istanbul, Turkey

### ABSTRACT

Sodium silicate ( $\text{Na}_2\text{Si}_3\text{O}_7$ ) also known as water glass is a very low cost material which is used in many industrial applications such as a builder in detergents, as a binder and adhesive etc. But so far the electrical properties of sodium silicate and its ability to screen radiation have never been investigated. In the present study, the frequency dependent electrical properties and gamma-ray shielding performance of water glass based bismuth oxide composites have been studied for the first time. In accordance with this purpose,  $\text{Na}_2\text{Si}_3\text{O}_7/\text{Bi}_2\text{O}_3$  glassy composites have been prepared for searching their possible applications in electronics and radiation screening. The surface morphology of the samples have been determined by Scanning Electron Microscope (SEM). The frequency dependent electrical properties such as complex impedance, complex dielectric function and conductivity have been analyzed at room temperature between 1 and 40 MHz. As a result of alternative current (ac) electrical analysis, it has been determined that the  $\text{Na}_2\text{Si}_3\text{O}_7/\text{Bi}_2\text{O}_3$  composites can be utilized as a dielectric layer in capacitors. On the other hand, since bismuth oxide is an anti-radiative material, the gamma-ray screening parameters such as mass attenuation coefficient, half layer and tenth layer values along with mean free path of the composites have been defined experimentally by using NaI(Tl) scintillation detector for the Ba-133 radiation source at 81 and 356 keV. The values of these parameters have also been checked by Monte-Carlo simulation. Since a good agreement has been assigned between experimental and Monte-Carlo simulation results, the related gamma ray shielding parameters have been determined by Monte-Carlo simulation for other gamma photon energies (140 keV, 208 keV, 468 keV, and 661 keV) which are generated from Tc-99, Lu-177, Ir-132, and Cs-137 sources. Ultimately,  $\text{Na}_2\text{Si}_3\text{O}_7/\text{Bi}_2\text{O}_3$  (35%) composite has been suggested as an eco-friendly, lead-free glassy structured material for the gamma radiation shielding in medical applications.

### ARTICLE HISTORY

Received 5 November 2018  
Accepted 23 January 2019

### KEYWORDS

Water glass; bismuth oxide; capacitor; gamma-ray screening; Monte-Carlo simulation; dielectric properties

## 1. Introduction

Sodium silicate also is known as glass water contains sodium oxide and silicon dioxide that form a glassy structure with being soluble in water. A low-cost water glass is used

**CONTACT** Zeynep Güven Özdemir  [zgozdemir@gmail.com](mailto:zgozdemir@gmail.com); [zguven@yildiz.edu.tr](mailto:zguven@yildiz.edu.tr); [zguvenozdemir@yahoo.com](mailto:zguvenozdemir@yahoo.com)

in industry as adhesives, detergents, ingredients in cleaning compounds, binders and etc. Although soluble silicates are currently used to solve efficiently and economically many problems arising in different branches of industry, their potential applications in dielectric and radiation shielding areas have not been adequately investigated until now.

As is known, glassy structures have become a very important material family for many electronic applications. While glassy structures with low dielectric constant are utilized as a dielectric layer in semiconducting packaging; high dielectric constant glasses are used in high energy capacitors (1–4). The number of investigation about the dielectric properties of silicate based glassy structures is very limited. Hsieh et al. studied the correlation between the chemical structure of sodium aluminosilicate (SAS) glasses and their dielectric constant. They achieved to increase the dielectric constant of SAS with increasing aluminum content in the SAS glass (5). Balaya et al. also studied the change of dielectric constant and electrical conductivity of lead silicate ( $\text{PbO-SiO}_2$ ) due to the addition of different modifiers such as  $\text{Na}_2\text{O}$ ,  $\text{K}_2\text{O}$ , and  $\text{BaO}$ . They have found that the silicate glasses with highest dielectric constant ( $\epsilon'$ ) and lowest dispersion ( $\Delta\epsilon'$ ) with frequency can be obtained with the highest concentrations of  $\text{Na}_2\text{O}$ ,  $\text{BaO}$ ,  $\text{PbO}$ ,  $\text{SiO}_2$  and the lowest concentration of  $\text{K}_2\text{O}$  (6). Morsi et al. researched the dielectric properties of 15%  $\text{Na}_2\text{O}$ , 20%  $\text{CaO}$  and 65% $\text{SiO}_2$  glasses doped with low contents of  $\text{Gd}_2\text{O}_3$ . The sample with the highest  $\text{Gd}_2\text{O}_3$  additive mole of  $0.83 \times 10^{-2}$  per 100 g glass exhibited the highest dielectric constant value for energy storage applications (7). Recently, Salehizadeh et al. tried to improve the dielectric properties of silicate glasses by embedding  $\text{Fe}_2\text{O}_3$  nano particles in the  $\text{SiO}_2$  glassy matrix. They obtained the highest dielectric constant for the sample containing 20% iron oxide nano particle (8). On the other hand, the dielectric properties of sodium silicate/bismuth oxide composites have not been investigated in the scientific literature. From this point of view, this study was devoted to prepare sodium silicate/bismuth oxide composites and determination of their electrical conductivity and dielectric parameters. Bismuth oxide was preferred as the additive for sodium silicate glass because of the broad application fields including optics, electronics, and nuclear technology of heavy glasses that often contain bismuth and/or lead. As is known, the heavy metal oxide based glasses such as bismuth oxide have attracted the attention of the scientific community due to their significant applications in nuclear radiation protection. Nuclear radiation protection can be achieved by shielding the radiation with screening materials. The increasing usage of  $\gamma$ -ray isotopes in many business lines including agriculture, medicine, industry, environment etc. has forced to produce shielding materials which are non-toxic and low cost. Therefore, developing new lead-free shielding glasses which exhibit approximately equivalent or beyond radiation shielding performance with lead are always necessary research field for studying.

Some recent studies related to the radiation shielding ability of the glasses containing bismuth oxide can be summarized as follows. Singh et al. have produced  $\text{Bi}_2\text{O}_3\text{-PbO-B}_2\text{O}_3$  glass systems by melt quenching technique and the radiation shielding properties of  $\text{Bi}_2\text{O}_3\text{-PbO-B}_2\text{O}_3$  glass systems are also better than concretes with the added advantage of being transparent to visible light (9). Also, Kaewkhao et al. investigated the use of bismuth oxide additives to improve the ability of glasses to shield against gamma rays. It is being reported that the radiation shielding properties were found to be improved with increasing  $\text{Bi}_2\text{O}_3$  concentration (10) as in other studies (11–13). Therefore,  $\text{Bi}_2\text{O}_3$  is found to be a very promising compound for glasses as potential shielding materials to improve the radiation shielding effectiveness. In this context, the radiation shielding ability of the

sodium silicate/bismuth oxide composites have also been determined experimentally and theoretically in the present study.

## 2. Theoretical background

In this section, the fundamental principles of impedance spectroscopy, frequency dependent electrical parameters, the main radiation shielding parameters and the basis of Monte-Carlo simulation have been summarized.

### 2.1. Fundamentals of impedance spectroscopy

The frequency dependence of the electrical properties of the samples has been determined by impedance spectroscopy technique. In this method, the complex impedance function ( $Z^*$ ) and the phase angle ( $\phi$ ) between  $Z^*$  and the real axis are measured. By using these frequency dependent variables, it is possible to calculate the real and imaginary components of the complex impedance ( $Z'$  and  $Z''$ ), complex dielectric function ( $\varepsilon'$  and  $\varepsilon''$ ), alternative current (ac) conductivity ( $\sigma_{ac}$ ) and etc. These parameters are defined in the following equations

$$Z' = Z^* \cos \phi \quad (1)$$

$$Z'' = Z^* \sin \phi \quad (2)$$

$$\varepsilon' = -Z'' \left[ \omega C_c (Z'^2 + Z''^2) \right]^{-1} \quad (3)$$

$$\varepsilon'' = Z' \left[ \omega C_c (Z'^2 + Z''^2) \right]^{-1} \quad (4)$$

$$\sigma_{ac} = \omega \varepsilon_0 \varepsilon'' \quad (5)$$

where  $\omega$ ,  $C_c$  and  $\varepsilon_0$  are angular frequency, the capacitance of empty measuring cell, and dielectric constant of free space, respectively.

### 2.2. General radiation shielding parameters

The radiation shielding parameters depend on the type of material and radiation. In order to determine the shielding ability of a material, some parameters must be determined. The mass attenuation coefficient ( $\mu_m$ ) is one of the most significant parameters for characterizing the diffusion and penetration of  $\gamma$ -rays in shielding product. The coefficients can be extracted by Lambert law;

$$\mu_m = \frac{\ln(I_0/I)}{\rho t} \quad (6)$$

where  $\rho$  is the density of the material ( $\text{g/cm}^3$ ),  $I_0$  and  $I$  correspond to the incident and transmitted intensities, respectively. In Equation (6)  $t$  is the thickness of an absorber (cm). It is beneficial to clarify the attenuation of  $\gamma$ -ray in terms of another parameter which is the half-value layer (HVL). This parameter is the thickness, at which the transmitted intensity is

reduced by 50% of the initial intensity. The half-value layer also displays the fact that energetic photons possess an ability to permeate the absorber as radiation energy raises. The *HVL* can be computed utilizing the following relation;

$$HVL = \frac{\ln 2}{\mu} \quad (7)$$

here  $\mu$  is the linear attenuation coefficient (which is equal to the multiplication of density of a material and mass attenuation coefficient). In addition, the mean free path ( $\lambda$ ) of the present composites can be determined by Equation (8)

$$\lambda = \frac{1}{\mu} \quad (8)$$

### 3. Experimental

#### 3.1. Preparation of the composites

The  $\text{Na}_2\text{Si}_3\text{O}_7$  solution with purity  $\geq 99\%$  (CAS #: 1344-09-8) has been supplied from Bal-mumcu Chemistry (Turkey).  $\text{Bi}_2\text{O}_3$  powder with a purity of 99.999% (CAS #:1304-76-3) was purchased from Sigma Aldrich (USA).

The composites have been prepared by mixing water glass ( $\text{Na}_2\text{Si}_3\text{O}_7$ ) solution with different mass of  $\text{Bi}_2\text{O}_3$  powder. Each time, 10 ml (or equivalently 12.9 g) water glass solution has been used for the preparation of the composites. While the pure  $\text{Na}_2\text{Si}_3\text{O}_7$  glassy structure has been prepared by using 10 ml  $\text{Na}_2\text{Si}_3\text{O}_7$  solution, the composites which contain 12%, 25% and 35%  $\text{Bi}_2\text{O}_3$  additive have been prepared by mixing 10 ml water glass solution and 1 g, 2.5 g and 4 g bismuth oxide, respectively. The mixtures including pure water glass solution have been mixed by a magnetic stirrer for twenty minutes. Then the resultant mixtures have been casted into a circular teflon mold with the diameter of 52 mm. Then the samples have been left to dry in teflon molds for seven days at room temperature. At the

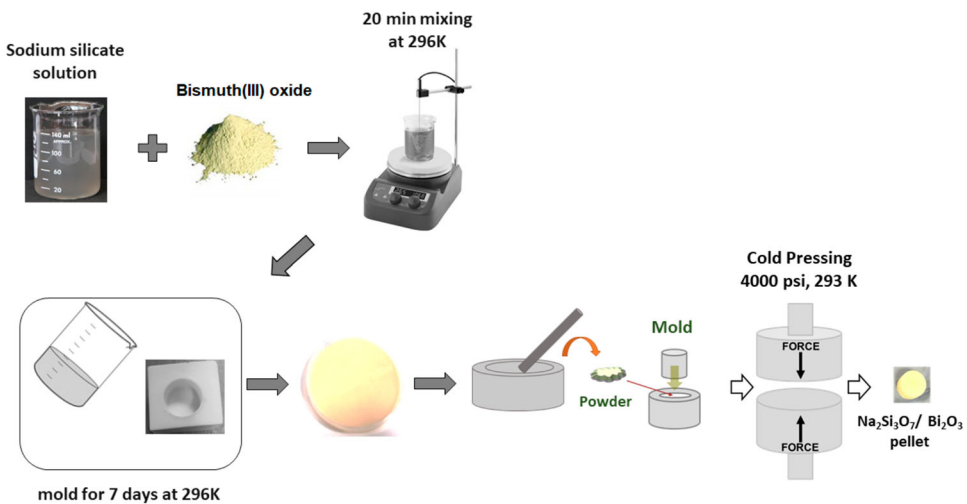


**Figure 1.** The physical appearance of the (a) water glass and (b) water glass/bismuth oxide composite.

**Table 1.** The mass density, the mass amount of water glass and bismuth oxide in gram units of the samples.

Sample	Mass amount (g)		Density (g/cm <sup>3</sup> )
	Bi <sub>2</sub> O <sub>3</sub>	Na <sub>2</sub> Si <sub>3</sub> O <sub>7</sub>	
Na <sub>2</sub> Si <sub>3</sub> O <sub>7</sub>	—	7.6	1.93 ± 0.16
Na <sub>2</sub> Si <sub>3</sub> O <sub>7</sub> /%12 Bi <sub>2</sub> O <sub>3</sub>	1	7.6	2.13 ± 0.07
Na <sub>2</sub> Si <sub>3</sub> O <sub>7</sub> /%25 Bi <sub>2</sub> O <sub>3</sub>	2.5	7.6	2.36 ± 0.11
Na <sub>2</sub> Si <sub>3</sub> O <sub>7</sub> /%35 Bi <sub>2</sub> O <sub>3</sub>	4	7.6	2.60 ± 0.12

end of seven days, the samples turned into a glassy structure as shown in Figure 1. Additionally, 5.3 g of mass loss has been measured for each sample due to the evaporation process during seven days. The thickness of the samples were varying between 1.6 and 1.9 mm. The mass densities of the samples have also been determined with Archimedes' principle by using water as an immersion liquid. The mass amounts in gram units of Na<sub>2</sub>Si<sub>3</sub>O<sub>7</sub> and bismuth oxide along with the mass densities have been summarized in Table 1.

Finally, to obtain homogenous distribution of bismuth oxide in the sodium silicate for each composite, the samples in the pellet form have been ground in an agate mortar for fifteen minutes and then the resultant homogenous fine powder has been pressed into a pellet under the pressure of 4000 Psi.

### 3.2. Scanning electron microscopy analysis of the composites

The surface morphology of a disk-shaped samples has been investigated by Scanning Electron microscope model Zeiss Supra 40VP. The SEM micrographs of the pure sodium silicate and the 35% Bi<sub>2</sub>O<sub>3</sub> doped sodium silicate composite have been shown in Figure 2. As shown in Figure 2(a), sodium silicate is viewed as big clusters with random shaped. Also, some small swellings along with few pores were observed at the surface of the

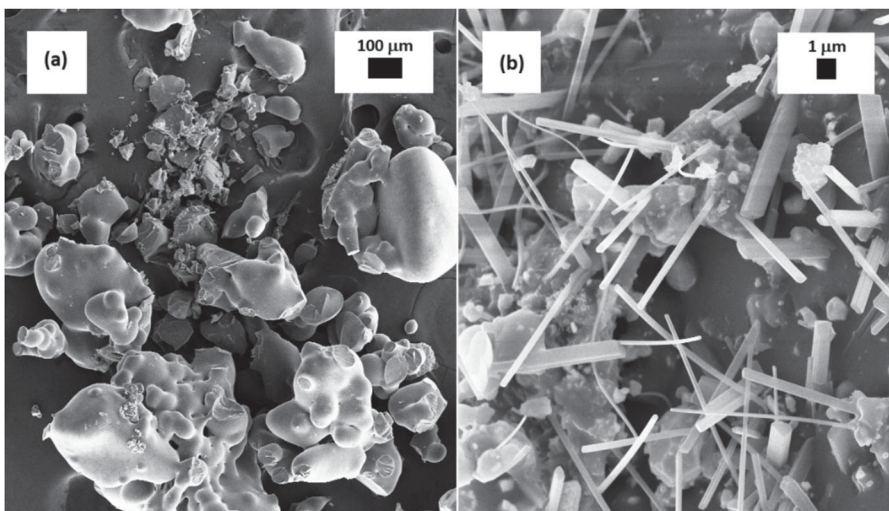


**Figure 2.** The SEM micrographs of (a) pure water glass and (b) Na<sub>2</sub>Si<sub>3</sub>O<sub>7</sub>/(35%)Bi<sub>2</sub>O<sub>3</sub> composite.

sodium silicate aggregates. Bismuth oxide additive was imaged as micron-sized rods and oblique rectangular prisms in the composite (See Figure 2(b)). While the length of the bismuth oxide rods was varying between 5–10  $\mu\text{m}$ , their diameters were determined between 0.15–0.50  $\mu\text{m}$ . Additionally, it was observed that the bismuth oxide additive is distributed almost homogeneously in the composite.

### 3.3. MCNP5

Radiation in space has quite complex stages in terms of progress and interaction with the material. For this reason, the calculation of the radiation interaction parameters by deterministic methods is very limited. By using Monte Carlo simulation, high accuracy results can be achieved by producing stochastic solutions instead of deterministic methods in accordance with the nature of radiation. MCNP – Monte Carlo N-particle – is of widespread use in modeling neutron, electron, photon or coupled neutron/electron/photon transport (14). In MCNP simulation, three-dimensional volumes are obtained by combining the various surfaces created and geometric setup stages are completed by assigning the desired materials and densities to these volumes.

In the present study, the MCNP Version 5 (MCNP5, released in 2003) has been used to calculate the total mass attenuation coefficients for Water Glass/ $\text{Bi}_2\text{O}_3$  composites. The interactions of photons with the glassy structures have been simulated using the Evaluated Nuclear Data Files (ENDF)/B-VI-Released 8 (15). The photo atomic data library MCPLIB04 was also utilized.

Figure 3, which was drawn by using MNCP Visual Editor Version 19L, shows the defined three-dimensional setup geometry in MCNP5 simulation code. In this work, the source has been defined in the mode card of the MCNP5 input file as a spherical with a diameter of 2 mm, source of photon and towards the detector. The cylindrical shaped NaI detector has the diameter of 2 cm. Also, it has been collimated with lead to prevent scattering and secondary particles. The sample materials were defined in material card of the input file as

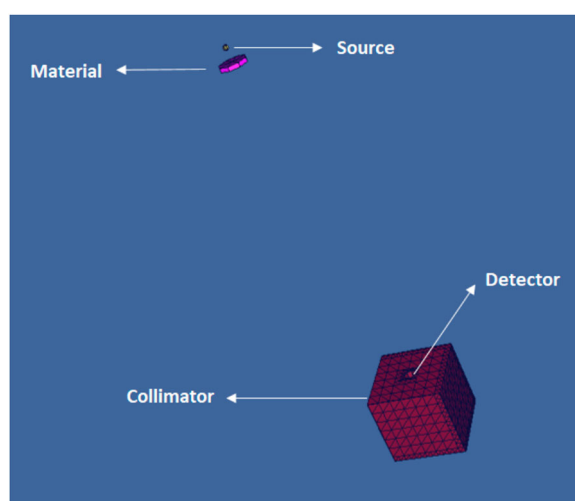


**Figure 3.** Monte Carlo simulation geometry.

**Table 2.** The material card of the input file of the samples for MCNP5 calculations.

Sample	Element (%)				Density (g/cm <sup>3</sup> )
	Na	O	Si	Bi	
Na <sub>2</sub> Si <sub>3</sub> O <sub>7</sub>	32.21	8.75	59.04	—	1.93
Na <sub>2</sub> Si <sub>3</sub> O <sub>7</sub> /%12 Bi <sub>2</sub> O <sub>3</sub>	28.47	8.93	52.17	10.43	2.13
Na <sub>2</sub> Si <sub>3</sub> O <sub>7</sub> /%25 Bi <sub>2</sub> O <sub>3</sub>	24.24	9.13	44.43	22.21	2.36
Na <sub>2</sub> Si <sub>3</sub> O <sub>7</sub> /%35 Bi <sub>2</sub> O <sub>3</sub>	21.10	9.28	38.68	30.93	2.60

shown in Table 2. As seen in Figure 3, composite has been located between the source and detector surface. MCNP5 simulations were run by using Intel® Core™ i5 -3317U CPU 1.70 GHz computer hardware. F4 tally, which gives the sum of average flux in the cell, was utilized to get intensity amounts in the detection area. For the simulation process, at first, the simulation code was run without shielding material. After that, the MCNP5 code was run with certain composites thickness. Each simulation was performed with 10<sup>8</sup> histories to keep the error below %0.05. Then, the mass attenuation coefficient of the shielding material ( $\mu/\rho$ ) can be calculated by using transmission factor of any type of composite,  $T(E, d)$  for electromagnetic radiation with energy,  $E$ , through the thickness,  $d$  (cm), of the shielding sample.  $T(E, d)$  is calculated by Equation (9)

$$T(E, d) = \frac{\Phi(E, d)}{\Phi(E, 0)} \quad (9)$$

where  $\Phi(E, d)$  is the average flux of photon with energy  $E$  in the volume of detector, which is passing through the composite with the thickness  $d$ .  $\Phi(E, 0)$  also is the average flux of the photon with energy  $E$  in the volume of detector which is radiated from the source.

## 4. Results and discussions

### 4.1. Electrical properties of the samples for electronic applications

The frequency dependent electrical measurements have been performed by NOVO Control Broadband Dielectric/Impedance analyzers with Quatro Cryosystem at room temperature between 1 Hz–40 MHz frequency. The samples with the shape of a cylindrical disk have been placed between two gold electrodes. The surface areas of the gold electrodes were 6.283 cm<sup>2</sup>.

The frequency dependences of the real and imaginary parts of the complex dielectric function of the samples have been shown in Figure 4(a) and (b), respectively. As shown in Figure 4(a), the real component of complex dielectric function has strong frequency dependence for all samples and all samples exhibit a decreasing  $\epsilon'$  values with increasing frequency for the low and mid-frequency regions. Additionally, pure water glass has the highest  $\epsilon'$  values at low frequencies. On the other hand, as the bismuth oxide additive concentration increases in the composite, the real part of the complex dielectric function decreases considerably between 1 Hz and  $5 \times 10^5$  Hz. However, it has been observed that the decrease of  $\epsilon'$  due to Bi<sub>2</sub>O<sub>3</sub> additive becomes insignificant above 35% bismuth oxide doping. In this context, almost the same  $\epsilon'$  values for 25% and 35% Bi<sub>2</sub>O<sub>3</sub> doping at each frequency can be interpreted that the dipole orientation with the applied electric field has become difficult.



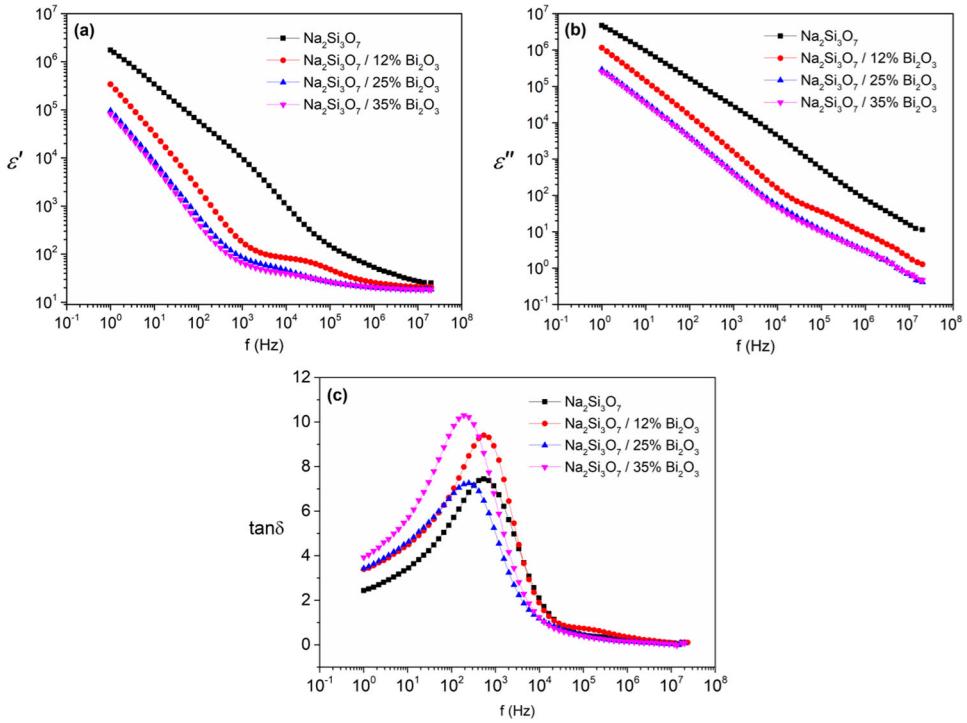


**Figure 4.** The frequency dependence of the (a) real and (b) imaginary components of the complex dielectric function and (c) dielectric loss spectra of the samples.

Moreover, the general behavior of the  $\epsilon'$  versus frequency curves indicates that the dielectric materials have layered structure which is known as Koop's model. In his phenomenological model, the dielectric material consists of two different regions in the context of their conductivity abilities. While grains have good conductivity, grain boundaries, which surround the grains, display poor conductivity. On the other hand, the high  $\epsilon'$  values observed at low frequency is due to high grain boundary resistance. Furthermore, dielectric relaxation strength ( $\Delta\epsilon$ ) given in Equation (10) have been calculated by determining  $\epsilon_\infty$  and  $\epsilon_s$  values from Figure 4(a).

$$\Delta\epsilon = \epsilon_s - \epsilon_\infty \quad (10)$$

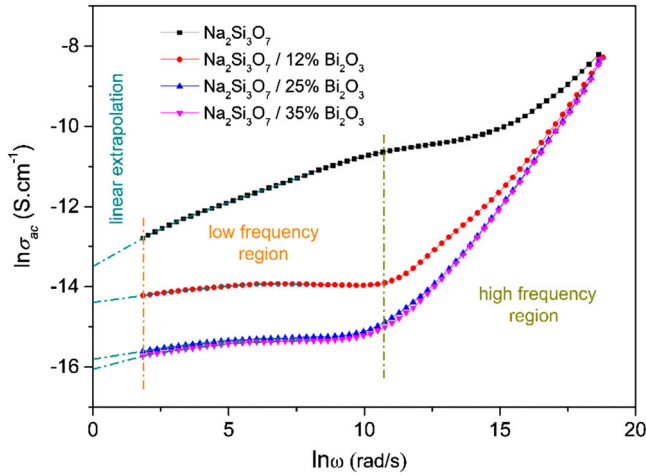
where  $\epsilon_\infty$  and  $\epsilon_s$  are the high and low limiting frequency dielectric constants, respectively. The related dielectric parameters have been given in Table 3. As shown in Table 3, dielectric relaxation strength decreased considerably with increasing bismuth oxide additive. From this point of view, one can deduce that the decrease of dielectric relaxation strength due to bismuth oxide doping makes the electric dipole orientation harder. In other words, the decrease in dielectric strength can be interpreted that bismuth oxide additive particles are less polar than sodium silicate.

When the effect of the bismuth oxide additive on sodium silicate's dielectric loss is investigated, it has been observed that the  $\epsilon''$  also decreases as the bismuth oxide additive increases (See Figure 4(b)). It is interesting to note that the  $\epsilon''$  has been considerably



**Table 3.**  $\varepsilon_s$ ,  $\varepsilon_\infty$ ,  $\Delta\varepsilon$  and  $f_r$  dielectric parameters of the samples.

Sample	$\varepsilon_s$	$\varepsilon_\infty$	$\Delta\varepsilon$	$f_r$ (Hz)
$\text{Na}_2\text{Si}_3\text{O}_7$	1737789	25	1737764	556
$\text{Na}_2\text{Si}_3\text{O}_7$ / 12% $\text{Bi}_2\text{O}_3$	347223	21	347202	525
$\text{Na}_2\text{Si}_3\text{O}_7$ / 25% $\text{Bi}_2\text{O}_3$	93833	19	93814	232
$\text{Na}_2\text{Si}_3\text{O}_7$ / 35% $\text{Bi}_2\text{O}_3$	80684	18	80666	195

**Figure 5.** The frequency dependence of the ac conductivity of the samples.

reduced with the increase of  $\text{Bi}_2\text{O}_3$  and it takes its minimum value for 25%  $\text{Bi}_2\text{O}_3$  additive. On the other hand, the reduced dispersion in  $\varepsilon''$  versus frequency curves observed in Figure 4(b) is an indicator of the decreasing values of dc conductivity. In Figure 4(c), the dielectric loss spectra of the samples have been shown. As shown in Table 3, the dielectric loss spectra of all samples have been characterized by a relaxation peak appearing at a characteristic frequency called as relaxation frequency,  $f_r$ . The existence of these peaks suggested the presence of relaxing dipoles in all our samples. The strength and frequency of relaxation also depend on the characteristic property of dipolar relaxation. Additionally, the tangent loss peaks shifted towards the lower frequency region as the bismuth oxide additive concentration increases in the sodium silicate.

The influence of bismuth oxide additive on alternative current (ac) conductivity ( $\sigma_{ac}$ ) of sodium silicate has also been discussed in the context of the real part of complex conductivity. Ac conductivity has been calculated by Equation (11)

$$\sigma_{ac} = \varepsilon_0 \varepsilon'' \omega = \sigma_{dc} + A\omega^s \quad (11)$$

where  $\varepsilon_0$  and  $\omega$  are the permittivity of free space and angular frequency, respectively. The  $\ln \sigma_{ac}$  versus  $\ln \omega$  curves have been shown in Figure 5. The angular frequency dependence of the conductivity of the samples has been discussed in the context of Universal Power Law (UPL) suggested by Jonscher (16). According to Jonscher's UPL, conductivity is composed of two parts: direct current (dc) and ac. While dc conductivity corresponds to the conductivity observed at  $\omega = 0$  and ac conductivity obeys power law where  $A$  is coefficient and ' $s$ ' is the frequency exponent. The frequency exponent is calculated by the slopes of  $\ln \sigma_{ac}$  versus

**Table 4.** The dc conductivity along with the low and high frequency  $s$  parameters values of the samples.

Sample	$\sigma_{dc} (\Omega m)^{-1}$	$s_{LF}$	$s_{HF}$
Na <sub>2</sub> Si <sub>3</sub> O <sub>7</sub>	$1.381 \times 10^{-6}$	0.239	0.292
Na <sub>2</sub> Si <sub>3</sub> O <sub>7</sub> / %12 Bi <sub>2</sub> O <sub>3</sub>	$5.621 \times 10^{-7}$	0.024	0.709
Na <sub>2</sub> Si <sub>3</sub> O <sub>7</sub> / %25 Bi <sub>2</sub> O <sub>3</sub>	$1.362 \times 10^{-7}$	0.051	0.840
Na <sub>2</sub> Si <sub>3</sub> O <sub>7</sub> / %35 Bi <sub>2</sub> O <sub>3</sub>	$1.064 \times 10^{-7}$	0.051	0.854

In  $\omega$  curve. In the context of UPL, dc conductivity ( $\sigma_{dc}$ ) and frequency exponents for the low and high-frequency sides have been determined and they summarized in Table 4.

As is clearly observed that bismuth oxide additive decreased the conductivity considerably. The  $s$  parameter values which are close to zero at low frequencies for the samples containing high bismuth oxide additive revealed that Bi<sub>2</sub>O<sub>3</sub> dopant makes the sodium silicate's conductivity frequency independent at the related frequency band. On the other hand, since  $s$  parameter takes values between 0.7 and 1 at high frequencies for the composites, the charge transport mechanism in the composites can be associated with the quantum tunneling process and/or correlated barrier hopping mechanism (17).

## 4.2. Gamma-Ray shielding ability of the samples

### 4.2.1. Experimental results

Mass attenuation coefficient which is one the most important parameter for determining gamma ray shielding ability of the samples has been calculated experimentally by measuring the attenuated and un-attenuated peaks emitted from the targets that have been detected by a 3''  $\times$  3'' NaI(Tl) detector. The model of the NaI(Tl) detector was 905-4 Ortec-Amtek.

The photomultiplier tube (PMT) base, digiBASE (Ortec) has 6.3 cm diameter and 8.0 cm length. The FWHM was equal to 46 keV at 662 keV and 65 keV at 1330 keV. PMT was separated from the NaI crystal by a 5 mm thick glass window. The data which were analyzed by the Maestro software collected into 2048 channels of the MCA. The gamma ray absorption performances of the samples were determined for 81 and 356 keV  $\gamma$ -rays emitted from a Ba-133 point radioactive source by measuring attenuated and un-attenuated intensities.

The mass attenuation coefficients ( $\mu/\rho$ ) of the samples have been calculated by the transmission method according to Lambert-Beer's law. The  $\mu/\rho$  values of the pure water glass and water glass/bismuth oxide for the photon energies of 81 and 356 keV have been shown in Figure 6. As shown in Figure 6, the mass attenuation coefficient decreases with the increase in photon energy from 81 keV to 356 keV. Observing such decrease in  $\mu/\rho$  values for the higher energetic gamma rays mostly probably indicate that the dominant interaction between gamma-ray and the glasses is Compton effect since the photoelectric effect is dominant for low energy photons (18). Moreover, the  $\mu/\rho$  value of pure Na<sub>2</sub>Si<sub>3</sub>O<sub>7</sub> at 356 keV has been determined as 0.996 cm<sup>2</sup>g<sup>-1</sup> which is in good agreement with the  $\mu/\rho$  values of Na (0.0963 cm<sup>2</sup>g<sup>-1</sup>), Si (0.1010 cm<sup>2</sup>g<sup>-1</sup>) and O (0.1000 cm<sup>2</sup>g<sup>-1</sup>) at 356 keV (19).

According to these experimental results given in Figure 6, the gamma-ray shielding performance of water glass was increased about 2.65 and 1.76 times for 35% Bi<sub>2</sub>O<sub>3</sub> additive at 81 and 356 keV, respectively. From this point of view, one can deduce that incorporation of bismuth oxide in the sodium silicate glass enhances the gamma ray shielding

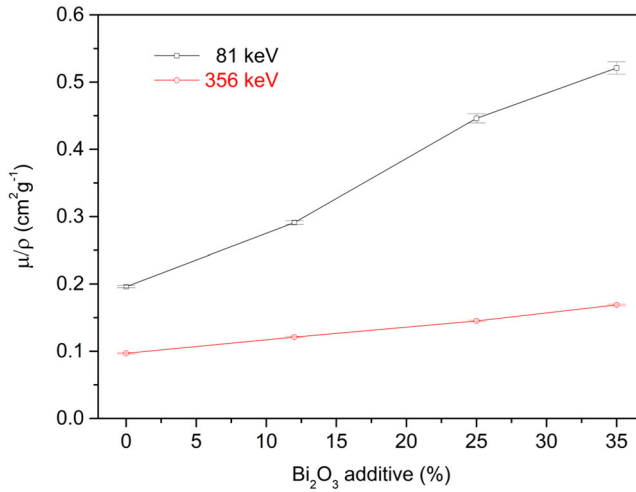


**Figure 6.** The variation of the mass attenuation coefficient of water glass with the increasing  $\text{Bi}_2\text{O}_3$  additive for 81 and 356 keV.

**Table 5.** HVL, TVL and  $\lambda$  parameters of the samples for the gamma photons with 81 and 356 keV energies.

Sample	HVL (cm)	TVL (cm)	$\lambda$ (cm)
$\text{Na}_2\text{Si}_3\text{O}_7$ (81 keV)	1.835	6.098	2.648
$\text{Na}_2\text{Si}_3\text{O}_7$ / %12 $\text{Bi}_2\text{O}_3$ (81 keV)	1.117	3.712	1.612
$\text{Na}_2\text{Si}_3\text{O}_7$ / %25 $\text{Bi}_2\text{O}_3$ (81 keV)	0.659	2.189	0.951
$\text{Na}_2\text{Si}_3\text{O}_7$ / %35 $\text{Bi}_2\text{O}_3$ (81 keV)	0.513	1.703	0.740
$\text{Na}_2\text{Si}_3\text{O}_7$ (356 keV)	3.724	12.373	5.373
$\text{Na}_2\text{Si}_3\text{O}_7$ / %12 $\text{Bi}_2\text{O}_3$ (356 keV)	2.677	8.894	3.863
$\text{Na}_2\text{Si}_3\text{O}_7$ / %25 $\text{Bi}_2\text{O}_3$ (356 keV)	2.023	6.720	2.919
$\text{Na}_2\text{Si}_3\text{O}_7$ / %35 $\text{Bi}_2\text{O}_3$ (356 keV)	1.580	5.251	2.281

ability considerably. The experimental  $\mu/\rho$  value of  $0.169 \text{ cm}^2\text{g}^{-1}$  for  $\text{Na}_2\text{Si}_3\text{O}_7/35\% \text{ Bi}_2\text{O}_3$  composite at 356 keV is also higher than the  $\mu/\rho (=0.115 \text{ cm}^2\text{g}^{-1})$  value of lead-free 25%(BaO)–20%(ZnO)–55%( $\text{B}_2\text{O}_3$ ) glass at the same energy level (20).

Other important parameters such as HVL, TVL and  $\lambda$  for producing radiation shielding material with a suitable composition have been shown in Table 5. As shown in Table 5, HVL, TVL, and  $\lambda$  parameters decreased considerably with the  $\text{Bi}_2\text{O}_3$  additive. The increase in the  $\gamma$ -ray mass attenuation coefficient and the decrease in the HVL of the water glass due to increasing  $\text{Bi}_2\text{O}_3$  additive can be associated with the hierarchical replacement of sodium silicate by  $\text{Bi}_2\text{O}_3$  because the  $\gamma$ -ray mass attenuation coefficient of bismuth is higher than that of silicon (19). Additionally, if an ordinary concrete's HVL (2.95 cm) and TVL (9.79 cm) thicknesses at 356 keV (21) are compared with the composites' HVL and TVL values, it is seen that even the composite with the lowest bismuth oxide doping performs better radiation shielding than the concrete. Of course, the highest  $\text{Bi}_2\text{O}_3$  doped water glass composite has the best gamma ray shielding performance for the gamma photons at 356 keV (See Table 5).

Observation of such a significant decrease in HVL, TVL and  $\lambda$  parameters of sodium silicate due to increasing bismuth oxide doping revealed that these composites have a

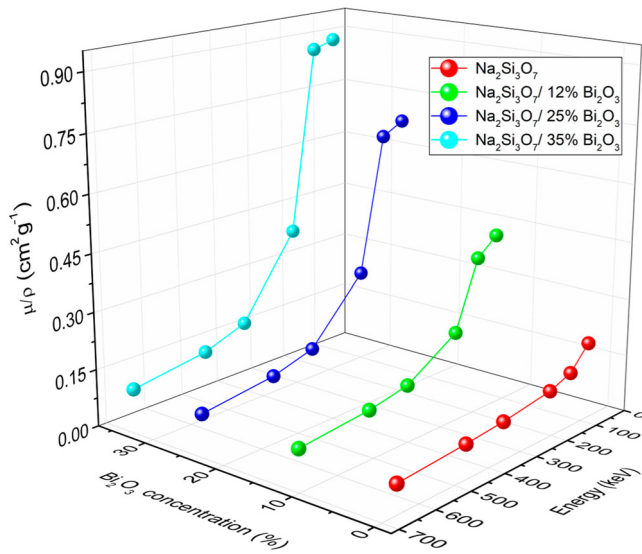


**Figure 8.** The change in the mass attenuation coefficients determined by MCNP5 and experiments of the water glass/bismuth oxide composites for the photon energy between 81 and 661 keV.

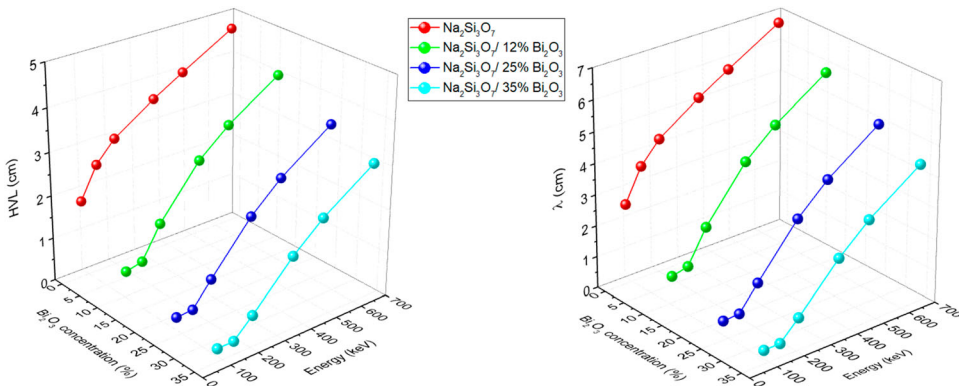


**Figure 9.** The change in (a) HVL and (b) mean free path ( $\lambda$ ) determined by MCNP5 and experiments of the water glass/bismuth oxide composites for the photon energy between 81 and 661 keV.

It should also be emphasized that the mass attenuation coefficient of the  $\text{Na}_2\text{Si}_3\text{O}_7/35\% \text{Bi}_2\text{O}_3$  glassy composite ( $=0.0873 \text{ cm}^2\text{g}^{-1}$ ) for 661 keV is slightly higher than the reported  $\mu/\rho$  values for ordinary concrete ( $=0.0792 \text{ cm}^2\text{g}^{-1}$ ) (22) and barite concrete ( $=0.078 \text{ cm}^2\text{g}^{-1}$ ) (23,24). Additionally, the  $\text{Na}_2\text{Si}_3\text{O}_7/35\% \text{Bi}_2\text{O}_3$  composite has almost equal  $\mu/\rho$  coefficient value at 662 keV with the 30%  $\text{Bi}_2\text{O}_3/70\% \text{B}_2\text{O}_3$  borate glasses (25).

The variation of HVL and mean free path with both bismuth oxide additive wt.% and gamma-ray energies ranging from 81 keV to 661 keV have also been given in Figure 9(a) and (b), respectively. According to Figure 9, it is worth mentioning that HVL and mean free path lengths obtained by MCNP5 decreased with the increment of bismuth oxide additive concentration and increased for higher photon energies. These characteristics of HVL and  $\lambda$  are also consistent with our experimental data shown in Table 5. Hence, the  $\text{Na}_2\text{Si}_3\text{O}_7/35\%$

$\text{Bi}_2\text{O}_3$  composite, which has the minimum HVL and mean free path values along with the maximum mass attenuation coefficients for each photon energies, can be considered the best gamma ray shielding material among the glassy structures prepared in this study.

## 5. Conclusions

In summary, the dielectric and gamma-ray shielding properties of sodium silicate/bismuth oxide glasses with different  $\text{Bi}_2\text{O}_3$  content have been investigated in the present study. While the dielectric parameters of the samples have been determined experimentally by using impedance analyzer, the gamma ray shielding performance of the samples has been tested both experimentally and MCNP5 simulation. According to the dielectric analysis of the samples, it has been suggested that  $\text{Na}_2\text{Si}_3\text{O}_7/35\% \text{Bi}_2\text{O}_3$  composite can be utilized as a dielectric layer in capacitors due to its high dielectric constant and low dielectric loss. The gamma-ray shielding ability of the samples has been determined experimentally for the gamma rays with the energies of 81 and 356 keV which are emitted from the Ba-133 point radiation source. Primarily, it has been observed that the mass attenuation coefficient increased with increasing bismuth oxide additive whereas HVL, TVL and  $\lambda$  decreased. Gamma-ray spectroscopy experiments also revealed that again  $\text{Na}_2\text{Si}_3\text{O}_7/35\% \text{Bi}_2\text{O}_3$  composite has the highest mass attenuation coefficient, the lowest HVL, TVL and mean free path for the both energies. Additionally, even the composite which contains the lowest  $\text{Bi}_2\text{O}_3$  additive exhibited better radiation shielding performance than the concrete. The same radiation shielding parameters have also been calculated by MCNP simulation for the gamma photons with the energies of 81 and 356 keV. By comparing the results of gamma-ray shielding experiments and MCNP5 simulation, it has been found that  $\mu/\rho$  values are in good agreement. Based on this agreement, the MCNP5 simulation has been utilized for determining the gamma ray shielding performance of the same samples against gamma photons with different energies which has not been experimentally tested. The last simulation has been performed for the gamma photon energies of 140, 208, 468 and 661 keV which are commonly used in medical applications. It has been determined that the  $\text{Na}_2\text{Si}_3\text{O}_7/35\% \text{Bi}_2\text{O}_3$  composite has again the minimum HVL and mean free path values along with the maximum mass attenuation coefficients for each photon energies. Ultimately, it has been come out that the composite with the highest bismuth oxide additive content has a great application potential in both electronics and radiation shielding areas.

## Acknowledgments

All author would like to thank Dr. Hilal Acar Demir for her assistance about Monte Carlo calculations.

## Disclosure statement

No potential conflict of interest was reported by the authors.

## Funding

This work was supported by Yildiz Technical University Scientific Research Projects Coordination Department under Project number: 2015-01-01-KAP06. Yaşar Karabul, one of the authors of the paper, was also supported by The Scientific and Technological Research Council of Turkey TUBITAK 2228 scholarship program.

## ORCID

Zeynep Güven Özdemir  <http://orcid.org/0000-0001-5085-5814>

## References

- (1) Geiger, G. Glass in Electronic Packaging Applications. *Am. Ceram. Soc. Bull.* **1990**, *69* (7), 1131–1136.
- (2) Kobayashi, K. DTA and MOS Characteristics for PbO-B<sub>2</sub>O<sub>3</sub>-SiO<sub>2</sub>-GeO<sub>2</sub> Passivation Glasses. *J. Non. Cryst. Solids* **1989**, *109* (2–3), 277–279.
- (3) Nair, K.M. *Glasses for Electronic Applications*; American Ceramic Society: Orlando, FL, 1991.
- (4) Tummala, R.R. Ceramic and Glass-Ceramic Packaging in the 1990s. *J. Am. Ceram. Soc.* **1991**, *74* (5), 895–908.
- (5) Hsieh, C.H.; Jain, H.; Kamitsos, E.I. Correlation Between Dielectric Constant and Chemical Structure of Sodium Silicate Glasses. *J. Appl. Phys.* **1996**, *80* (3), 1704–1712.
- (6) Balaya, P.; Shrikhande, V.K.; Kothiyal, G.P.; Goyal, P.S. Dielectric and Conductivity Studies on Lead Silicate Glasses Having Mixed Alkali and Alkaline Earth Metal Oxides. *Curr. Sci.* **2004**, *86* (4), 553–556.
- (7) Morsi, R.M.M.; El-Ghany, S.I.A.; Morsi, M.M. Electrical Properties of Silicate Glasses of Low Level Gadolinium Oxide Doping Including Dielectric and Infrared Measures. *J. Mater. Sci. Mater. Electron.* **2015**, *26* (3), 1419–1426.
- (8) Salehizadeh, S.A.; Graça, M.P.F.; Valente, M.A. Effect of Iron on the Dielectric Properties of Silicate Glasses Prepared by Sol-gel. *Phys. Status Solidi* **2014**, *11* (9–10), 1455–1458.
- (9) Singh, N.; Singh, K.J.; Singh, K.; Singh, H. Comparative Study of Lead Borate and Bismuth Lead Borate Glass Systems as Gamma-Radiation Shielding Materials. *Nucl. Instruments Methods Phys. Res. Sect. B Beam Interact. with Mater. Atoms* **2004**, *225* (3), 305–309.
- (10) Kaewkhao, J.; Kirdsirir, K.; Limkitjaroenporn, P.; Limsuwan, P.; Jeongmin, P.; Kim, H. Interaction of 662 KeV Gamma-Rays with Bismuth-Based Glass Matrices. *J. Korean Phys. Soc.* **2011**, *59*, 661–665.
- (11) Singh, V.P.; Badiger, N.M.; Chanthima, N.; Kaewkhao, J. Evaluation of Gamma-Ray Exposure Buildup Factors and Neutron Shielding for Bismuth Borosilicate Glasses. *Radiat. Phys. Chem.* **2014**, *98*, 14–21.
- (12) Yao, Y.; Zhang, X.; Li, M.; Yang, R.; Jiang, T.; Lv, J. Investigation of Gamma Ray Shielding Efficiency and Mechanical Performances of Concrete Shields Containing Bismuth Oxide as an Environmentally Friendly Additive. *Radiat. Phys. Chem.* **2016**, *127*, 188–193.
- (13) Mariyappan, M.; Marimuthu, K.; Sayyed, M.I.; Dong, M.G.; Kara, U. Effect Bi<sub>2</sub>O<sub>3</sub> on the Physical, Structural and Radiation Shielding Properties of Er<sup>3+</sup> Ions Doped Bismuth Sodiumfluoroborate Glasses. *J. Non. Cryst. Solids* **2018**, *499*, 75–85.
- (14) Briesmeister, J.F. MCNP – A General Monte Carlo N-Particle Transport Code. *Los Alamos Natl. Lab.* **2000**, *March*, 1–10.
- (15) White, M.C. Photoatomic Data Library MCPLIB04: A New Photoatomic Library Based on Data From ENDF/B-VI Release 8, LANL Internal Memorandum X-5: MCW-02-111 and LA-UR-03-1019, 2002.
- (16) Jonscher, A.K. A New Understanding of the Dielectric Relaxation of Solids. *J. Mater. Sci.* **1981**, *16* (8), 2037–2060.
- (17) Elliott, S.R.A.C. Conduction in Amorphous Chalcogenide and Pnictide Semiconductors. *Adv. Phys.* **1987**, *36* (2), 135–217.
- (18) Issa, S.A.M. Effective Atomic Number and Mass Attenuation Coefficient of PbO–BaO–B<sub>2</sub>O<sub>3</sub> Glass System. *Radiat. Phys. Chem.* **2016**, *120*, 33–37.
- (19) Mostafa, A.G.; Saudi, H.A.; Hassaan, M.Y.; Salem, S.M.; Mohammad, S.S. Studies on the Shielding Properties of Transparent Glasses Prepared From Rice Husk Silica. *Am. J. Mod. Phys.* **2015**, *4* (4), 149–157.
- (20) Chanthima, N.; Kaewkhao, J.; Limkitjaroenporn, P.; Tuscharoen, S.; Kothan, S.; Tungjai, M.; Kaewjaeng, S.; Sarachai, S.; Limsuwan, P. Development of BaO–ZnO–B<sub>2</sub>O<sub>3</sub> Glasses as a Radiation Shielding Material. *Radiat. Phys. Chem.* **2017**, *137*, 72–77.

- (21) Biswas, R.; Sahadath, H.; Mollah, A.S.; Huq, M.F. Calculation of Gamma-Ray Attenuation Parameters for Locally Developed Shielding Material: Polyboron. *J. Radiat. Res. Appl. Sci.* **2016**, *9* (1), 26–34.
- (22) Stanković, S.J.; Ilić, R.D.; Janković, K.; Bojović, D.; Lončar, B. Gamma Radiation Absorption Characteristics of Concrete with Components of Different Type Materials. *Acta Phys. Pol. A* **2010**, *117* (5), 812–816.
- (23) Singh, K.J.; Singh, N.; Kaundal, R.S.; Singh, K. Gamma-Ray Shielding and Structural Properties of PbO–SiO<sub>2</sub> Glasses. *Nucl. Instruments Methods Phys. Res. Sect. B Beam Interact. with Mater. Atoms* **2008**, *266* (6), 944–948.
- (24) Kaur, K.; Singh, K.J.; Anand, V. Correlation of Gamma Ray Shielding and Structural Properties of PbO–BaO–P<sub>2</sub>O<sub>5</sub> Glass System. *Nucl. Eng. Des.* **2015**, *285*, 31–38.
- (25) Singh, K.; Singh, H.; Sharma, V.; Nathuram, R.; Khanna, A.; Kumar, R.; Singh Bhatti, S.; Singh Sahota, H. Gamma-Ray Attenuation Coefficients in Bismuth Borate Glasses. *Nucl. Instruments Methods Phys. Res. Sect. B Beam Interact. with Mater. Atoms* **2002**, *194* (1), 1–6.